

**Mo-99 2014 TOPICAL MEETING ON  
MOLYBDENUM-99 TECHNOLOGICAL DEVELOPMENT**

June 24-27, 2014  
Hamilton Crowne Plaza  
Washington D. C.

**Overview of Argonne support for Mo-99 medical isotope  
production: NorthStar Medical Technologies**

Sergey Chemerisov<sup>a</sup>, George Vandegrift<sup>a</sup>, Gregory Dale<sup>b</sup>, Peter Tkac<sup>a</sup>, Roman Gromov<sup>a</sup>, Vakh  
Makarashvili<sup>a</sup>, Bradley Micklich<sup>a</sup>, Charles Jonah<sup>a</sup>, Thad Heltemes<sup>a</sup>, David Rotsch<sup>a</sup>, Keith A.  
Woloshun<sup>b</sup>, Michael Holloway<sup>b</sup>, Frank Romero<sup>b</sup> and James Harvey<sup>c</sup>

<sup>a</sup>Argonne National Laboratory, 9700 South Cass Avenue, Argonne, IL 60439,

<sup>b</sup>Los Alamos National Laboratory, P.O. Box 1663, Los Alamos, NM 87545,

<sup>c</sup>NorthStar Medical Technologies, LLC, 5249 Femrite Drive, Madison, WI 53718

**ABSTRACT**

Argonne National Laboratory (Argonne) and Los Alamos National Laboratory (LANL) are supporting NorthStar Medical Technologies in their efforts to become a domestic <sup>99</sup>Mo producer. NorthStar Medical Technologies is utilizing the accelerator production technology pathway for the production of <sup>99</sup>Mo using a photonuclear reaction <sup>100</sup>Mo( $\gamma$ ,n)<sup>99</sup>Mo in an enriched <sup>100</sup>Mo target. So far we have performed six demonstration of the <sup>99</sup>Mo production, with natural and enriched <sup>100</sup>Mo, utilizing liquid (water) and gaseous-He cooling. Those experiments have demonstrated the production of the <sup>99</sup>Mo at relatively high beam power on the target and effective separation of the <sup>99m</sup>Tc from low-specific-activity Mo targets. Following a completion of the upgrade to the Argonne electron linear accelerator, we are conducting a series of thermal and production experiments with three different enriched-<sup>100</sup>Mo target disks and at higher power and at different beam energies to optimize <sup>99</sup>Mo production. Other investigations include calculations for development of the facility shielding requirements, design of the beam-transport components, beam diagnostic, components reliability studies, and enriched molybdenum recovery and purification. This presentation will review the current status of the project.

## 1. Introduction

The National Nuclear Security Administration's (NNSA's) Global Threat Reduction Initiative (GTRI), in partnership with commercial entities and the US national laboratories, is working to accelerate development of a reliable domestic supply of  $^{99}\text{Mo}$  for nuclear medicine while also minimizing the civilian use of highly enriched uranium (HEU). This summary describes the activities performed at Argonne National Laboratory (Argonne) in collaboration with Los Alamos National Laboratory (LANL) and NorthStar Medical Technologies, LLC that support the accelerator-technology pathway for the production of  $^{99}\text{Mo}$  using a photonuclear reaction  $^{100}\text{Mo}(\gamma,n)^{99}\text{Mo}$  in an enriched  $^{100}\text{Mo}$  target. A plot of the photonuclear cross section for this reaction is shown in Figure 1. The threshold for the reaction is 9 MeV. The maximum cross section is 150 mb at 14.5 MeV.

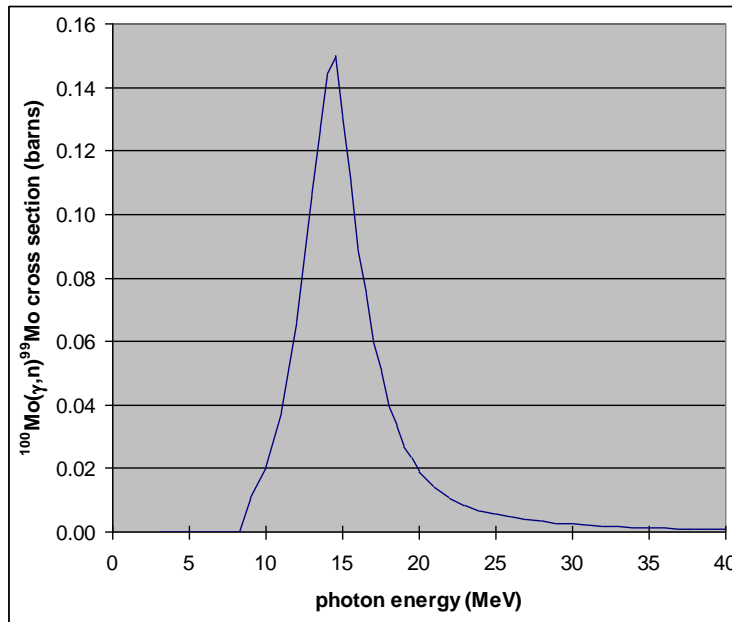


Figure 1. Photonuclear cross section for the  $^{100}\text{Mo}(\gamma,n)^{99}\text{Mo}$  reaction.

In this approach, a high-power electron accelerator is used to produce the required flux of high-energy photons through the bremsstrahlung process. So far, we have performed six demonstrations of  $^{99}\text{Mo}$  production, with natural and enriched  $^{100}\text{Mo}$ , utilizing liquid (water) and gaseous He cooling. Those experiments have demonstrated production of the  $^{99}\text{Mo}$  at relatively high beam power on the target and effective separation of the  $^{99\text{m}}\text{Tc}$  from low-specific-activity Mo targets.

## 2. Summary of experiments

Due to the small photon cross section for the reaction and the high cost of the enriched  $^{100}\text{Mo}$  material, one would want to use the highest photon flux available. That leads to a high thermal load on the target. Most of the heat deposited on the target is dissipated in the first centimeter of the target material, while production of the  $^{99}\text{Mo}$  is distributed more evenly. The ability to remove heat from the target is a limiting factor in the production of  $^{99}\text{Mo}$ . The first three demonstrations of the  $^{99}\text{Mo}$  production with natural and enriched  $^{100}\text{Mo}$  used water

as the coolant. While those experiments demonstrated production of the  $^{99}\text{Mo}$  at relatively low beam power on the target and effective separation of the  $^{99\text{m}}\text{Tc}$  from low specific activity targets, they also pointed out limitations of water cooling due to corrosion/erosion of the Mo target under high radiation fields.

To eliminate the problem associated with water cooling and extend the power envelope on the target, the decision was made to utilize gaseous He cooling. In March 2011, Argonne and LANL scientists successfully demonstrated the ability to dissipate up to 1 kW power per 12-mm-diameter 1-mm-thick (~1 g) disks using a He once-through flow system with 300 cf/min flow. Because 23 tanks of He were emptied in ~20 minutes, this method of cooling limited the time of the irradiation. To (1) extend irradiation time and (2) demonstrate what would be used commercially, a closed-loop He-cooling system was developed. In late 2011, Argonne and LANL scientists successfully designed and built the closed-loop cooling system. A successful test of the system with up to 10 kW beam on the target was conducted in March 2012. In May 2014 we performed a second test of the target system at 42 and 35 MeV and achieved 15kW beam power on the target. This summer, we are planning to conduct five production runs at the Argonne linac facility. The test matrix for those production runs is summarized in Table 1.

Table 1. Test matrix for upcoming tests.

	Production Test 1	Production Test 2	Production Test 3	Production Test 4	Thermal Test	Production Test 5
Purpose	Test Enrichment 1 at high energy	Test Enrichment 2 at high energy	Test Enrichment 3 at high energy	Test Enrichment 2 at low energy	Validate the thermal performance of the target	Test Enrichment 4 at high energy for long duration
Energy (MeV)	42	42	42	35	42 and 35	42
Current (uA)	240	240	240	500	300 and 550	240
Power (kW)	21	21	21	17.5	12.6 and 19.3	21
Duration (hours)	24	24	24	24	2	156
Targets	E1 (97.39%) and Natural	E2 (99.03%) and Natural	E3 (95.08%) and Natural	E2 (99.03%) and Natural	Natural	E4 (95.08%) and Natural
Mo99 EOB Activity [Ci]	<b>5.4</b>	<b>5.3</b>	<b>5.3</b>	<b>9.6</b>	<b>0.2 and 0.28</b>	<b>19.2</b>
Target Thermocouples	No	No	No	No	Yes	No

### 3. Linac upgrades

According to the calculations, irradiation of the  $^{100}\text{Mo}$  target at higher energy would significantly increase the yield of  $^{99}\text{Mo}$ . A beam energy in the range 35-42 MeV seems to be optimum for the  $^{100}\text{Mo}(\gamma,n)^{99}\text{Mo}$  reaction. To achieve this beam energy, we have implemented a linac upgrade by installing two new accelerator structures and associated RF

equipment. The new accelerator structures for the linac upgrade were manufactured by MEVEX Corporation (Canada). Each of the accelerator structures is powered by a separate klystron-based modulator. During installation, we encountered difficulties in achieving the expected beam power and energy level. The problems were traced to the RF circulators provided as a part of the upgrade. Design of the RF circulators was faulty, leading to the excessive RF absorption at high power levels. After that, we obtained RF circulators from a different supplier that perform according to the specifications and allowed us to finish the upgrade. The upgraded accelerator is shown on Figure 2. The load lines for the upgrade accelerator are presented on Figure 3.



Figure 2. Upgraded electron linac at Argonne.

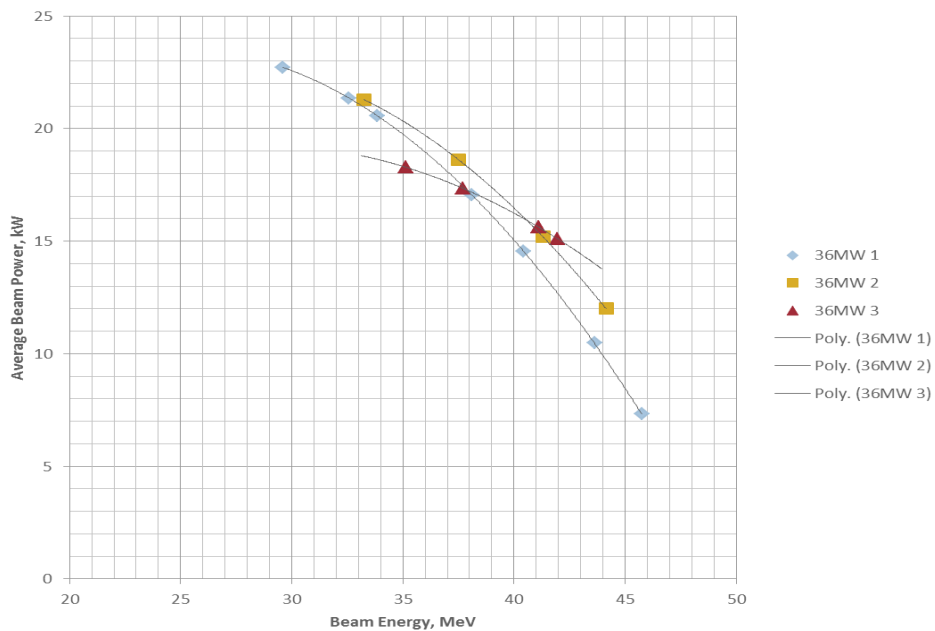


Figure 3. Performance of the upgraded linac.

Measurements of the linac performance have shown that we can achieve 12kW beam power at 42 MeV beam energy and 18kW at 35 MeV.

#### 4. Beam-line design for the production facility

The beam transport system is designed to deliver an electron beam from the accelerator to the target. In the proposed production facility, two linear accelerators will be used to irradiate a single target from the opposite sides to minimize the size of the target. Because of this arrangement, the beam line has to incorporate a bending magnet to eliminate direct line-of-sight for the two beam lines. The design of the beam line depends on the beam parameters (energy, energy spread, etc.) and target geometry. Elements of the beam-transport system should provide transportation, focusing, and positioning of the beam on the target surface. Main elements of the transport line shown in Figure 4 are a focusing-defocusing (FODO) doublet, a 10-degree bending magnet, and a raster magnet.

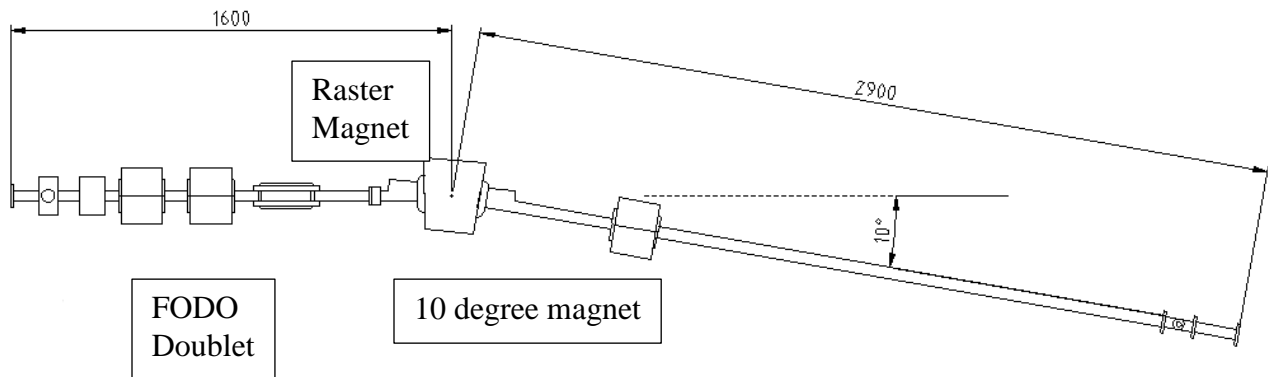


Figure 4. Proposed arrangement of the transport beamline. Distances are given in mm.

The pair of FODO quadrupoles is used to focus the beam. An additional quadrupole is installed after the 10-degree bending magnet to compensate for beam dispersion due to its energy spread. Since the target area is bigger than the transverse beam size, the raster magnet is to be used to evenly distribute the beam on the surface of the target. The last 2 meters of the beam line have no magnetic elements. This space is reserved to install concrete shielding for radiation protection.

To avoid the hysteresis problem, the raster magnet has no yoke. A prototype of the raster magnet consists of two pairs of rectangular shaped coils. Preliminary tests of this magnet were performed at the Van de Graaff accelerator at 3 MeV electron beam energy. The coils were powered by an AC current with an amplitude about 2.5A. The initial beam-spot diameter was about 0.3" when the raster magnet was off. The coils of the raster magnet were powered by the alternating current with a frequency at 21Hz. The coils were fed by a sinusoidal current; the vertical coils had the 90-degree phase shift. With these conditions, the

beam made a circular path across the target point with displacement of about 0.15" from the center. The resulting spot had an average diameter of about 0.6", with 15% of top roughness.

The existing linac's beamline is composed of several focusing quadrupoles, steering coils, and two 10-degree bending magnets (Figure 5). It is close to the designed beam line; therefore, the transport parameters are expected to be similar. In our tests, the accelerated beam with the energy of about 35MeV was directed to the 10-degree line. Efficiency of the transport was measured by beam-current monitors (BCM). One of them is installed between the FODO focusing quadrupoles and first 10-degree magnet, and the other is at a distance of about 3 meters after the 10-degree bending magnet. A water-cooled aperture with a 0.6" hole was installed before the second beam-current monitor. A comparison of pulse currents from the BCMs demonstrated good transport efficiency for the proposed beam line. The beam transport is close to 100% for the beam with an energy of 35MeV and energy spread up to +/- 0.8MeV.



Figure 5. LINAC beam line in experimental cell.

A prototype of the bending magnet was installed and tested on the existing linac 10-degree beam line. The uniformity of the magnetic field was good. It consumes power at less than 400W and does not require water cooling. Now it is used as a regular second bending magnet at the 10-degree beam line.



Figure 6. Prototype of the 10-degree bending magnet.

## 5. Molybdenum recycling

After the Mo-99 has decayed, the solution that was fed daily to the Technegen generator needs to be treated to recover valuable Mo-100 for future production of the Mo target. Therefore, recycle of Mo will require conversion of  $K_2MoO_4$  in 5 M KOH solution to  $MoO_3$  powder that can be further reduced to Mo metal. As part of the Mo recovery process, purification from several byproducts, such as Zr and Nb that are generated during the production of Mo-99 by  $(\gamma, n)$  reaction on the Mo-100 target, is necessary. However, the most challenging purification is the separation of Mo from potassium. The starting Mo-100 enriched material contains <100 mg of potassium in one kilogram of molybdenum. However, after dissolving the irradiated Mo-100 target in hydrogen peroxide and converting it to  $K_2MoO_4$  in 5 M KOH (0.2 g-Mo/mL), the solution contains about 1.8 kg of potassium per one kilogram of molybdenum. One requirement for the recycled Mo material is that the impurities in the recycled material need to be at the same level or below the concentration present in starting material to facilitate acceptance for use of recycled Mo-100 by the FDA (U.S. Food and Drug Administration). Therefore, the amount of potassium (K) in purified  $MoO_3$  powder should be below 100 mg of potassium per kilogram of molybdenum (required purification factor for removal of potassium is  $\sim 1 \times 10^5$ ) to prevent production of large amounts of K-42 during the irradiation of Mo-100 disks at the linac. Additionally, recycle of Mo requires conversion of  $K_2MoO_4$  in 5 M KOH solution to Mo metal powder with high Mo

recovery yields (>95%) due to a high cost of enriched Mo-100 material. The requirement for commercial recovery of Mo-100 material is the ability to process up to 400g of Mo on a daily basis.

Several reagents such as HNO<sub>3</sub>, H<sub>2</sub>SO<sub>4</sub>, acetic acid, and ethanol were investigated as potential candidates to precipitate Mo from highly alkaline solutions (5M KOH). HNO<sub>3</sub> and H<sub>2</sub>SO<sub>4</sub> are strong acids; therefore, an addition of these acids into highly alkaline solution causes a very exothermic neutralization reaction, and their use in the precipitation step is quite challenging. When ethanol is added into highly alkaline Mo solution, a white precipitate containing K<sub>2</sub>MoO<sub>4</sub> is formed. Although Mo losses in this step are minimal (<0.2%), additional reagent is necessary for removal of potassium from potassium molybdate. The benefit of using acetic acid (AcA) is that neutralization reaction is relatively mild; Mo losses are usually <1%; and up to 80% of K can be removed in precipitation step. However, the use of AcA by itself is not very effective for further removal of potassium. The most effective removal of potassium can be achieved when the Mo precipitation step with AcA is followed by multiple washes with concentrated nitric acid (70%). Also, very important is how well the Mo precipitate is mixed during the washing step with fresh HNO<sub>3</sub>. It was observed that prolonged mixing time can lead to more efficient removal of potassium. Small-scale experiments with ~1g of Mo showed very good Mo recoveries (95-100%) with the potassium concentration in the final MoO<sub>3</sub> product below 100mg-K/kg-Mo. More than 10 washes with nitric acid are needed to achieve this purification. Several large scale experiments with up to 200g of Mo were also performed using this procedure. Some optimization steps to improve Mo recoveries are being implemented. To process 400g of Mo, about 9 liters of acetic acid are needed for the precipitation step, and ~90 liters of 70% HNO<sub>3</sub> for washing steps. Most of the nitric acid can be recycled using rotary evaporation, where condensed nitric acid can be re-used, while potassium in the form of potassium nitrate is disposed as a solid waste.

## **5. Monte Carlo computer calculations for production facility and target**

We have performed some calculations on the bulk shielding requirements for the NorthStar accelerator-based Mo-99 production facility. The proposed facility layout is shown in Figure 7 below. We have estimated shielding requirements for regions above the production targets, in adjoining accelerator bays, and in the corridors outside the accelerator vaults. Shielding estimates take into account both photons and neutrons from the electron beam interactions with the molybdenum target.

The photon and neutron source terms were calculated for 42-MeV electrons incident on a 25-mm thick, 25.4-mm diameter target made of molybdenum. Any target structure and coolant were ignored for this calculation, providing a conservative estimate of the shielding required. Calculations were performed with version 2.7.0 of the radiation transport code MCNPX [1]. A geometric approximation was used to obtain rapid convergence of the solutions, which is challenging for these very thick shields. The shield was assumed to be spherically symmetric, and the photon spectrum for either zero or 90 degrees was used as the source term (depending on the shielding location being evaluated) into all angles. The total number of photons emitted from the source was adjusted to be the photon emission rate for the

appropriate direction (in photons/sr/s) multiplied by  $4\pi$ . The calculations also used exponential attenuation variance reduction along with cell- or mesh-based weight windows.



Figure 7. Elevation and plan views of the proposed Northstar Mo-99 production facility.

The main conclusion from this study is that most effective shielding will include combination of the lead and concrete. Tables 2 and 3 summarize the effectiveness of the shielding for 0 and 90 degree relative to the direction of the beam.

Table 2. Dose rate for primary and secondary radiations in shield of 30 cm lead + concrete for 120 kW of 42-MeV electrons incident on molybdenum. Calculations used the source term for  $0^\circ$  emission.

concrete thickness (cm)	neutron source		photon source		total dose rate (rem/hr)
	neutron dose rate (rem/hr)	photon dose rate (rem/hr)	neutron dose rate (rem/hr)	photon dose rate (rem/hr)	
150	3.84e-4	2.87e-3	2.65e-2	2.57e-1	2.87e-1
200	5.34e-6	1.15e-4	3.34e-4	1.02e-2	1.07e-2
250	8.50e-8	4.93e-6	4.56e-6	4.61e-4	4.71e-4

Table 3. Dose rate for primary and secondary radiations in shield of 30 cm lead + concrete for 240 kW of 42-MeV electrons incident on molybdenum. Calculations used the source term for 90° emission.

concrete thickness (cm)	neutron source		photon source		total dose rate (rem/hr)
	neutron dose rate (rem/hr)	photon dose rate (rem/hr)	neutron dose rate (rem/hr)	photon dose rate (rem/hr)	
100	8.74e+0	2.27e+1	5.32e-1	1.47e+0	3.34e+1
200	7.78e-4	1.70e-2	3.40e-5	9.49e-4	1.88e-2
250	8.88e-6	6.04e-4	3.42e-7	3.34e-5	6.46e-4

As one can see from the above tables a combination of 30 cm of lead and 250 cm of concrete provide adequate radiation shielding in the facility.

### References

[1] D. Pelowitz, ed., "MCNPX User's Manual, Version 2.7.0", LA-CP-11-00438, Los Alamos National Laboratory (April 2011).

### Acknowledgement

Work supported by the U.S. Department of Energy, National Nuclear Security Administration's (NNSA's) Office of Defense Nuclear Nonproliferation, under Contract DE-AC02-06CH11357. Argonne National Laboratory is operated for the U.S. Department of Energy by UChicago Argonne, LLC.